

Complex morphology and functional dynamics of vital murine intestinal mucosa revealed by autofluorescence 2-photon microscopy

Antje Klinger · Regina Orzekowsky-Schroeder ·
Dorthe von Smolinski · Maike Blessenohl · Anna Schueth ·
Norbert Koop · Gereon Huettmann · Andreas Gebert

Accepted: 7 December 2011 / Published online: 7 January 2012
© The Author(s) 2012. This article is published with open access at Springerlink.com

Abstract The mucosa of the gastrointestinal tract is a dynamic tissue composed of numerous cell types with complex cellular functions. Study of the vital intestinal mucosa has been hampered by lack of suitable model systems. We here present a novel animal model that enables highly resolved three-dimensional imaging of the vital murine intestine in anaesthetized mice. Using intravital autofluorescence 2-photon (A2P) microscopy we studied the choreographed interactions of enterocytes, goblet cells, enteroendocrine cells and brush cells with other cellular constituents of the small intestinal mucosa over several hours at a subcellular resolution and in three dimensions. Vigorously moving lymphoid cells and their interaction with constituent parts of the lamina propria were examined and quantitatively analyzed. Nuclear and

lectin staining permitted simultaneous characterization of autofluorescence and admitted dyes and yielded additional spectral information that is crucial to the interpretation of the complex intestinal mucosa. This novel intravital approach provides detailed insights into the physiology of the small intestine and especially opens a new window for investigating cellular dynamics under nearly physiological conditions.

Keywords Intravital two-photon microscopy · Small intestine · Mucosal architecture · Cellular migration

Introduction

The columnar epithelium of the small intestine consists mainly of enterocytes and few scattered goblet cells. Singly dispersed throughout the epithelium are enteroendocrine cells, secreting serotonin and peptide hormones and brush cells that are assumed to represent chemoreceptors of the digestive tract (Hoefer et al. 1996). The study of vital intestinal mucosa has failed in the past, due to the fact that once intestinal cells are removed from basement membrane and underlying stroma, apoptosis is initiated (Hall et al. 1994; Strater et al. 1995). Culture models of intestinal cells, while experimentally tractable, may not convincingly represent the *in vivo* situation because they generally lack interactions with the supporting tissues, including blood and lymph vessels, nerves and extracellular matrix.

Recent studies, using intravital imaging, even discuss factors uniquely relevant to intact tissue (Miller et al. 2002). These data assume that cell–cell interactions observed *in vitro* are quite different from those observed *in vivo*, since lymphatic and circulatory connections are disrupted in explanted preparations, generating unphysiological conditions

Electronic supplementary material The online version of this article (doi:10.1007/s00418-011-0905-0) contains supplementary material, which is available to authorized users.

A. Klinger (✉) · M. Blessenohl
Institute of Anatomy, University of Luebeck,
Ratzeburger Allee 160, 23538 Luebeck, Germany
e-mail: Aklinger@anat.uni-luebeck.de

R. Orzekowsky-Schroeder · N. Koop · G. Huettmann
Institute of Biomedical Optics, University of Luebeck,
Luebeck, Germany

D. von Smolinski
Institute of Veterinary Pathology, University of Berlin,
Berlin, Germany

A. Schueth
Department of Urology, University of Maastricht Medical
Centre, Maastricht, Netherlands

A. Gebert
Institute of Anatomy II, University of Jena, Jena, Germany

(Caldwell et al. 2001; Stoll et al. 2002; von Andrian 2002). In this study, we introduce intravital autofluorescence 2-photon (A2P) microscopy based on imaging of naturally occurring endogenous fluorophores such as NAD(P)H and FAD (Denk et al. 1990; Koenig 2000). This novel experimental approach enables the study of the intact intestinal tissue in living mice for up to 8 h, allowing the analysis of cell functions of all participating cells in epithelium and underlying lamina propria. Our approach offers significant advantages for physiological studies of the intestinal mucosa. Using a 40/1.2 water immersion objective, we produce optical sections of the intestinal mucosa at a 0.5-micron resolution, so that individual lysosomes and mitochondria can be easily distinguished. Differentiation of lysosomes and mitochondria was also achieved by fluorescence lifetime imaging microscopy (FLIM), a technique in which the mean fluorescence lifetime of a chromophore is measured at each spatially resolvable element of a microscope image (Skala et al. 2007). Since endocytic and lysosomal pathways play key roles in both the stimulation and implementation of immune responses (Harding et al. 1991; Tulp et al. 1994; Peters et al. 1995; Schmidt et al. 2009), the differentiation of individual cell organelles is necessary to access a complete view of cell composition.

The orchestration of cell migration, cell–cell interactions and intracellular signalling events is fundamental for achieving an accurate view of the physiologically intact intestinal mucosa. A2P microscopy affords an unparalleled view of single-cell spatiotemporal dynamics deep within the intact tissue and we show that individual migrating lymphocytes within the lamina propria can be tracked over several minutes. The application of fluorescent molecular markers, such as UEA-I FITC and organelle-specific dyes complements autofluorescence imaging and delivers additional information on structural characteristics.

The results, presented here not only permit the evaluation of cell physiology and cellular dynamics, but also provide morphological data of most, if not all tissue components in living intestinal mucosa. For the first time, the complex collaboration and organization of all involved cell types of the epithelium and underlying lamina propria is shown. In the present study, we demonstrate that A2P microscopy has the potential of becoming an important tool in multispectral imaging of cellular structure–function relationships and cellular migration in gastrointestinal microscopy. The results presented here open a wide range of interesting and powerful new applications for intravital imaging of the healthy and inflamed intestinal mucosa, evaluating various aspects of cell function, including cell vitality and apoptosis, paracellular permeability and particle transport, endocytosis and blood flow.

Materials and methods

Animal surgery

Female Balb/c mice ($n = 20$), 8–10 weeks of age, were purchased from Charles River Laboratories (Sulzfeld, Germany) and kept under standard conditions with free access to food and water. Animals were anaesthetized using a combination of Fentanyl (Bayer, Leverkusen Germany), Midazolam (Curamed, Karlsruhe, Germany) and Medetomidin (Pfizer, Karlsruhe, Germany) intraperitoneally. After assuring adequate anesthesia, the abdominal cavity was opened and an isolated ileal loop was prepared in situ without disturbing the blood supply. The loop was glued (3M Vetbond TissueAdhesive, St. Paul, MN, USA) on a heated metallic block and sliced so that the mucosa could be carefully pressed to a fixed microscopic cover slip to dampen movement artefacts, yet maintained tissue viability (Fig. 1). During all procedures, the small intestine was constantly moisturized with saline (37°C) and core body temperature was maintained at 37°C using a homeothermic table. The tissue was constantly perfused, as seen by erythrocyte movement phenomena, and cells remained fully motile with no evidence of decreased viability for experiments lasting up to 8 h. The animal experiments were approved by the local government (Ministerium für Umwelt, Naturschutz und Landwirtschaft Schleswig–Holstein V742-72241.122, TV-No. 23/p/04).

In vivo labeling with fluorescent probes

Hoechst 33258 (Sigma, Schnellendorf, Germany) was dissolved in saline and 200 μg was applied intraperitoneally or intravenously. The lectin Ulex europaeus conjugated to FITC (UEA-I FITC, 0.1 mg/ml, Sigma) was applied lumenally.

A2P image analysis

All imaging was conducted using the commercial imaging system JenLab DermaInspect 101 (JenLab, Jena, Germany) equipped with a tunable femtosecond Ti:sapphire laser (pulse width <100 fs, repetition frequency 80–90 MHz; Spectra Physics, Mountain View, CA, USA) using a 40 \times /1.2 water immersion objective (Zeiss, Jena, Germany). For imaging excitation wavelength was tuned between 710 and 920 nm. A2P imaging was typically done at excitation wavelength of 730 nm, which is known to mainly excite NAD(P)H (Huang et al. 2002) and emission was detected between 380 and 540 nm. Digital images covered a field of 150 \times 150 μm at a pixel size of 0.29 \times 0.29 μm . Repeated A2P recording of 2D images or 3D image stacks at intervals of 15–30 s resulted in time-lapse series displayed

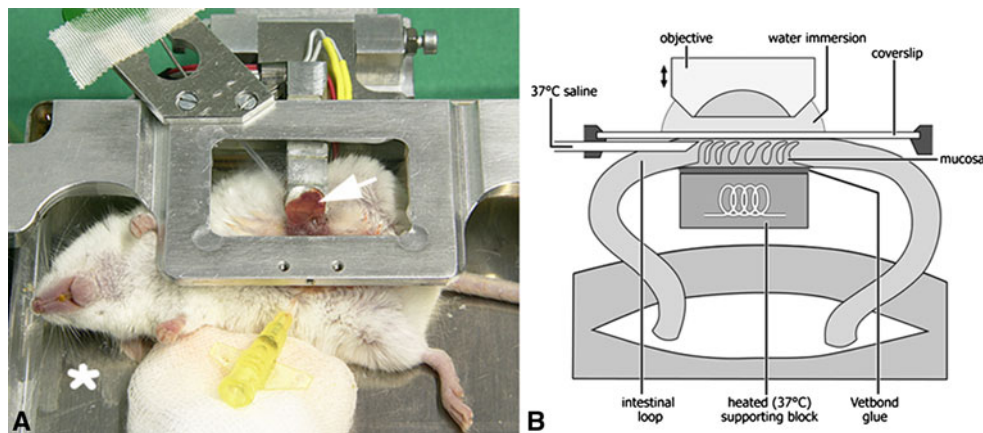


Fig. 1 Intravital 2-photon imaging system (a). Anaesthetized balb/c mouse on a homeothermic table (*asterisk*) with an exteriorized ileal loop (*arrow*) (b). Schematic diagram of the chamber for intravital imaging. The loop of the small intestine was glued on a heated

metallic block and sliced, so that the mucosa could be carefully pressed to a fixed cover slip to dampen movement artefacts. During all procedures, the small intestine was constantly moisturized with saline and core body temperature was maintained at 37°C

as movies over up to 60 min. Using time correlated single photon counting (TCSPC; Becker and Hickl, Berlin, Germany) we performed fluorescence lifetime imaging. A2P-stacks were processed using IMARIS software (Bitplane, Zurich, Switzerland) for three-dimensional analysis of mucosal morphology.

Lectin labeling and confocal laser scanning microscopy

Cryosections (10- μm thick) were fixed in a mixture of methanol and acetone for 10 min at -20°C and transferred to PBS. The sections were incubated with Ulex europaeus I lectin conjugated to FITC (UEA-I FITC, 0.1 mg/ml, Sigma) for 1 h. Nuclei were stained using Hoechst 33258 (0.1 $\mu\text{g}/\text{ml}$ in PBS for 1 h; Sigma). Controls were performed by preincubation of the lectin with fucose overnight. The lectin–gold labeling was performed in PBS containing 1.5% bovine serum albumin-c (BSA-c; Biotrend, Cologne, Germany) and 0.1% sodium azide. Free aldehyde groups were blocked for 15 min in a drop of this buffer (PBS-BSA) containing 0.7% L-lysine. After rinsing in PBS containing 5% bovine serum albumin (Serva; Heidelberg, Germany), 0.1% cold water fish skin gelatin (Biotrend), 1% normal goat serum (Sigma), and 0.05% Tween 20 (Serva), the sections were incubated with PBS-BSA containing the biotinylated Ulex europaeus I lectin at 4°C overnight. After rinsing, the grids were incubated for 4 h with a goat anti-biotin antibody (1:50) conjugated to 20-nm colloidal gold (BioCell; Cardiff, UK). Finally, the grids were treated with 2% glutaraldehyde in PBS, washed in distilled water, and stained with uranium acetate and lead citrate. The sections were examined in a Zeiss EM10 electron microscope (Zeiss; Oberkochen, Germany). Controls were carried out by omitting the lectin and by preincubating the lectin with fucose overnight. Cryosections of

lectin labelings were examined using a Zeiss LSM 510 UV meta confocal laser scanning microscope, equipped with lasers for 364, 488, 543, and 633 nm excitation (Zeiss, Jena, Germany). In addition to fluorescence channels, a differential interference contrast (DIC) image was recorded simultaneously.

Transmission electron microscopy

Tissue samples were fixed in a solution of 0.6% paraformaldehyde, 2% glutaraldehyde, and 2 mg/ml CaCl_2 in 0.1 M Na-cacodylate-HCl-buffer, pH 7.3, for 16 h. After being rinsed in cacodylate buffer for 30 min, the blocks were postfixed in 2% osmium tetroxide in cacodylate buffer, dehydrated in a graded series of ethanol dilutions, transferred to propylene oxide, and embedded in Araldit (Serva, Heidelberg, Germany) according to standard protocols. Semithin sections, 1 μm in thickness, were stained with toluidine blue. Ultrathin sections, 50–70 nm in thickness, were stained with uranium acetate and lead citrate and examined in a Philips EM400 electron microscope.

Results

In vivo histology of small intestinal epithelium

For A2P microscopy, mice were anaesthetized and a loop of small intestine was exposed for intravital imaging (Fig. 1a, b). Typical structures of living small intestinal mucosa were visualized at 20–25- μm depth using a 40/1.2 water immersion objective and excitation at 730 nm (Fig. 2a–c). We could clearly identify structural characteristics of enterocytes, goblet cells and enteroendocrine cells (EC) at high resolution and contrast. Cytosol and

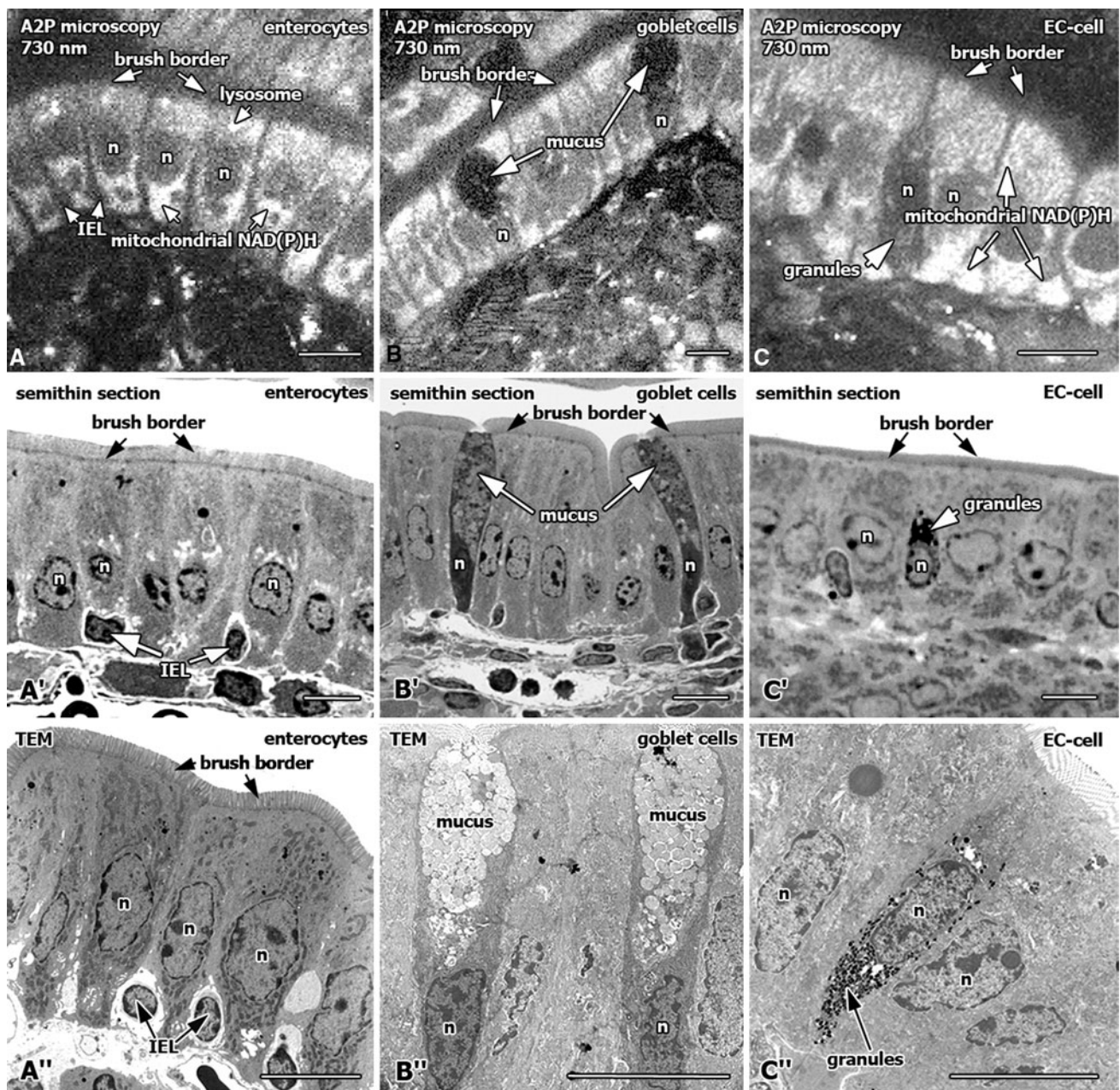


Fig. 2 A2P images of enterocytes (a), goblet cells (b) and enteroendocrine (EC-) cells (c) in the living mucosa of small intestine. Mitochondria, cytosol and lysosomes of most epithelial cells exhibited a strong signal when excited at 730 nm. Other cellular structures, such as nuclei (n), brush border, the mucus-containing granules of

goblet cells and the granules of EC-cells appeared *dark*. Intraepithelial lymphocytes (IEL) exhibited only a weak fluorescence. Visualization of *in vivo* mucosa morphology was in excellent agreement with histological observations in semithin sections (a'–c') and electron microscopic sections (a''–c''). (Scale bars, 10 μ m)

mitochondria of most epithelial cells exhibited a strong signal, while other cellular structures, such as nuclei, brush border, enteroendocrine cells and the mucus granules of goblet cells appeared *dark*. Since NAD(P)H is the main autofluorescent fluorophore observed using 2-photon 730-nm excitation (Bennett et al. 1996; Piston and Knobel 1999), bright cytoplasmic regions correspond to mitochondria, which are known to have a higher NAD(P)H

concentration than the remaining cytoplasm (Patterson et al. 2000). Lysosomes also exhibited a strong autofluorescence (Fig. 2a). Enteroendocrine cells were rarely seen and were identified by their typical slender and elongated shape (Fig. 2c). Comparison of these A2P intravital images to semithin and ultrathin sections revealed that the autofluorescence distribution aligns well with the histology of preserved intestinal mucosa.

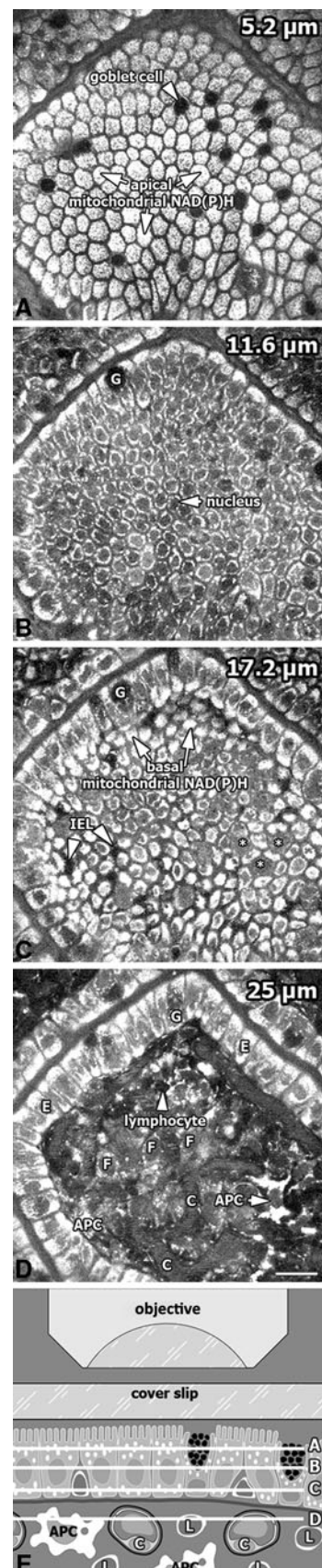
Fig. 3 A2P images of a 25- μm thick slice of mouse small intestinal mucosa excited at 730 nm. Stack of optical sections through a villus: **a** 5.2 μm below the tissue surface, mitochondrial NAD(P)H in the apical cytoplasm of enterocytes exhibited a strong signal. Mucus-containing goblet cells appeared *dark*. **b** In 11.6- μm depth, the image predominantly showed the nuclei of enterocytes. Goblet cell (G). **c** In 17.2- μm depth, a strong signal from the basal mitochondrial NAD(P)H was exhibited and the nuclei of goblet cells (*asterisk*) were identified. Intraepithelial lymphocytes appeared with *dark* nuclei between the enterocytes (*arrowheads*). Goblet cell (G). **d** In 25- μm depth, the underlying lamina propria with fibroblasts (F), capillaries (C) and lymphoid cells, such as lymphocytes (*arrowhead*) and antigen-presenting cells (APC, *arrow*) were identified. Enterocyte (E), goblet cell (G). **e** Schematic diagram of the four different focus planes (**a–d**). Lymphocytes (L), capillaries (C), antigen-presenting cell (APC) (Scale bar, 20 μm)

Three-dimensional architecture of small intestinal mucosa at a subcellular resolution

To investigate the complex architecture of intestinal mucosa, series of images were obtained at different depths within the tissue. Figure 3a–d, Online Resource, ESM_1.mpg shows representative images of the typical appearance of living intestinal mucosa at various depths at an excitation wavelength of 730 nm. In about 5- μm depth (Fig. 3a) beneath the tissue surface, enterocytes and goblet cells could be clearly identified and in about 12 μm beneath the tissue surface, dark nuclear regions appeared (Fig. 3b). NAD(P)H of mitochondria in the basal cytoplasm of enterocytes together with the nuclei of goblet cells and intraepithelial lymphocytes were visualized in about 17- μm depth (Fig. 3c). In about 25- μm depth (Fig. 3d), the epithelium and the lamina propria of intestinal mucosa could be clearly distinguished. The lamina propria, as a loose connective tissue, consists of abundant cells and ground substance. These cells were primarily lymphocytes, antigen-presenting cells (APCs) and fibroblasts. APCs are known to exhibit well-developed lysosomes and they displayed a strong signal in A2P imaging. We were able to verify intact microcirculation by erythrocyte movement phenomena (Data not shown). It was also possible to obtain 3D data sets by acquiring a focus series along the optical axis. Figure 4a–c shows a 3D rendering of a 25- μm thick image stack.

Lysosomes exhibit different characteristics than mitochondria in A2P microscopy

Since lysosomes play an important role in immune responses, it is necessary to differentiate them from other cell organelles. Lysosomal membranes contain flavin–adenine dinucleotide (FAD; Shin and Mego 1988) which can be efficiently excited at a wavelength of 800 nm in 2-photon microscopy (Fig. 5d) in contrast to NAD(P)H in mitochondria, which is best excited at wavelengths of 710–730 nm in nonlinear optics using femtosecond laser pulses. FAD may



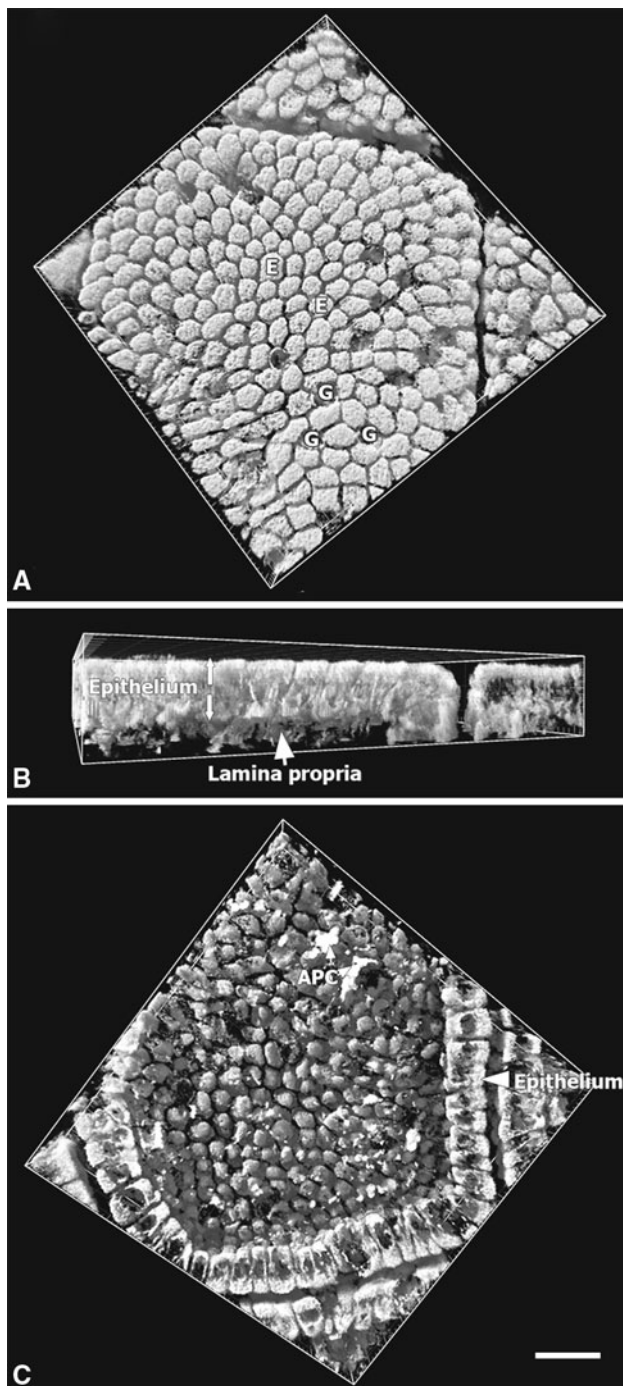


Fig. 4 3D rendering of a 25- μm -thick slice of mouse small intestine excited at 730 nm. Image represents a $150 \times 150 \times 25 \mu\text{m}$ volume of a villus area **a** view from the luminal side of a villus with strong mitochondrial NAD(P)H signal in enterocytes (E). Mucus-containing granules of goblet cells (G) appeared dark. **b** Lateral view of the epithelium and underlying lamina propria. **c** View from the lamina propria side, showing the mitochondrial NAD(P)H signal of the basal cytoplasm and antigen-presenting cells (APC) in the lamina propria. (Scale bar, 20 μm)

also be responsible for the faster fluorescence lifetime of lysosomes (~ 800 ps), in contrast to lifetimes of mitochondria ($\sim 1,200$ ps) (Fig. 5b, c). Lysosome signal can therefore be easily distinguished from NAD(P)H signal in mitochondria by excitation wavelength and fluorescence lifetime.

Fluorescence stains complement autofluorescence imaging in the small intestine

To visualize structural characteristics, such as microvilli of epithelial cells, molecular markers and fluorescent dyes were applied to the vital intestinal mucosa. Ulex europaeus agglutinin lectin I conjugated to FITC (UEA-I FITC), given intraluminally, specifically binds to α -L-fucose, which is located in the glycocalyx covering the microvilli of brush cells (Gebhard and Gebert 1999). Brush cells were singly dispersed throughout the epithelium and could also be identified by their bundles of microfilaments, which extend deep into the apical cytoplasm. These microfilaments appeared dark in intravital imaging (Fig. 6a). Comparison of UEA-I FITC intravital staining to ex vivo staining on cryosection (Fig. 6b) and ultrathin sections (Fig. 6c) revealed that intravital staining of brush cells with UEA-I FITC aligns well with that of preserved brush cells. Hoechst 33258 dye is a cell-permeant DNA-binding dye and, after intravenous injection, is distributed throughout the small intestine after application (Fig. 7, Online Resource ESM_2.mpg). Hoechst dye brightly labeled the nuclei of all participating cells in the epithelium of small intestinal mucosa as well as nuclei of circulating lymphocytes and other cells within the lamina propria (Fig. 7a–c).

Intravital imaging of motile cells in the lamina propria of small intestinal mucosa

To study the motility of cells within the lamina propria, nuclei were labeled with the nuclear Hoechst dye, which was injected intraperitoneally 24 h prior to intravital A2P microscopy. The nuclei of cells in the epithelium were only weakly stained, but some nuclei of cells in the lamina propria showed intense fluorescence. These nuclei were round and about 6 μm in diameter, vigorously moving and could easily be tracked over the time. We strongly suggest that these cells are lymphocytes which populate the lamina propria of the small intestinal mucosa in large numbers. To analyze the motility of stained cells, we acquired time-lapse 3D image series at 15-s intervals and tracked the spatial coordinates of individual lymphocytes. As shown in Fig. 8a–f, Online Resource ESM_3.mpg, these cells exhibited a crawling pattern of motility, as the leading edge of the cell probed and

Fig. 5 **a** A2P image of the epithelium of mouse small intestine excited at 730 nm. Lysosomes in the apical cytoplasm of enterocytes. **b** Corresponding color-coded fluorescence lifetime image of the apical cytoplasm of the epithelium. Lysosomes (*orange*) could be differed from mitochondria (*green*) by their fluorescence lifetime. **c** Lysosomes exhibited an average fluorescence lifetime of 810 ps (*arrow 1*), whereas lifetimes of mitochondria were longer with $\sim 1,230$ ps (*arrow 2*). **d** A2P image of the epithelium excited at 800 nm. At this excitation wavelength the signal source was dominated by lysosomes in the apical cytoplasm of enterocytes. **e** Electron microscopic section showing mitochondria and lysosomes in the apical cytoplasm of enterocytes, nuclei (*n*). (Scale bars **a, b, d** 10 μm ; **e**, 2 μm)

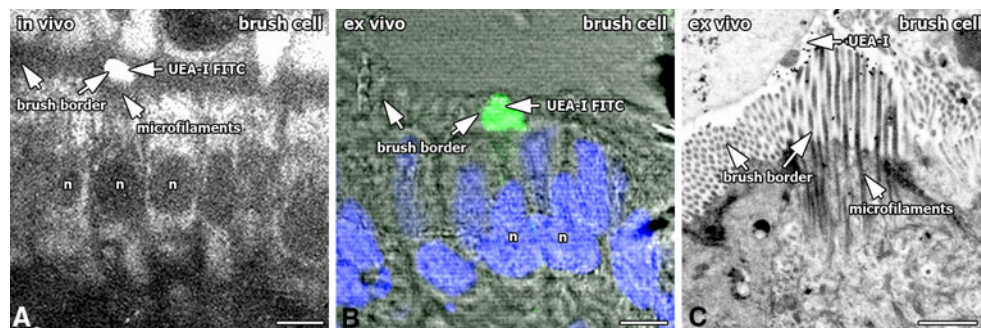
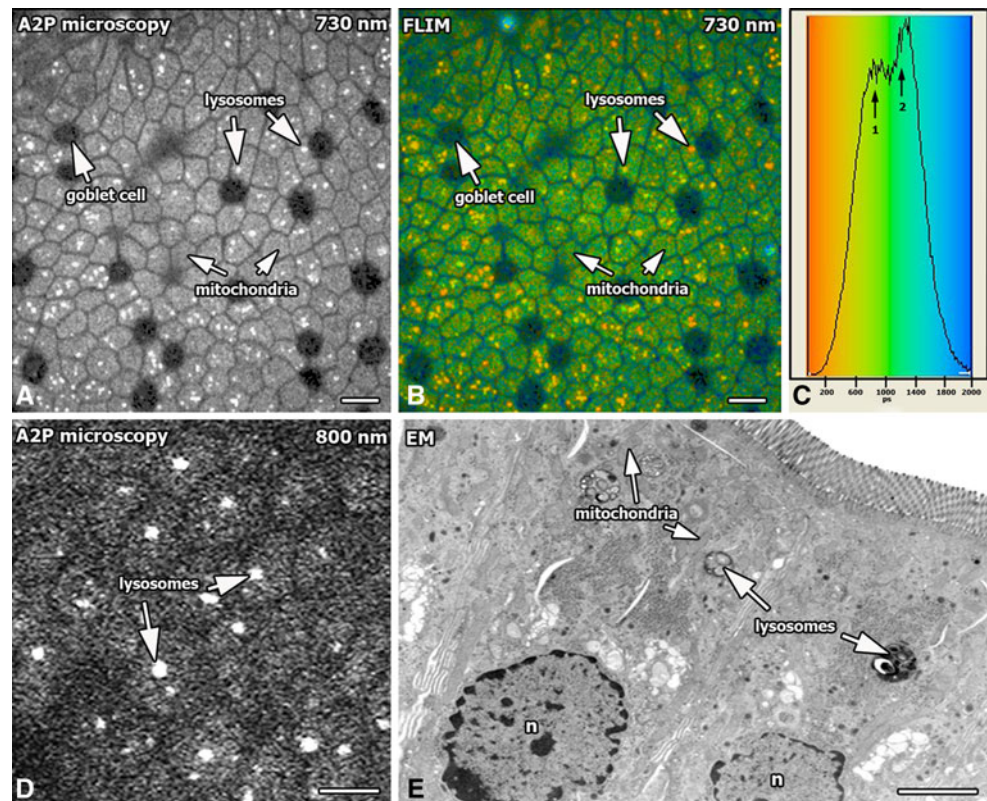


Fig. 6 **a** A2P image of the in vivo histology of brush cells in the epithelium of mouse small intestine excited at 730 nm. The brush border of brush cells, which usually appeared *dark* in A2P images could be successfully labeled in vivo by luminal application of the Ulex europaeus agglutinin lectin I conjugated to FITC (UEA-I FITC). The typical microfilament rootlet bundles of brush cells appeared *dark*. Nuclei (*n*). **b** Confocal laser scanning microscopy of tissue

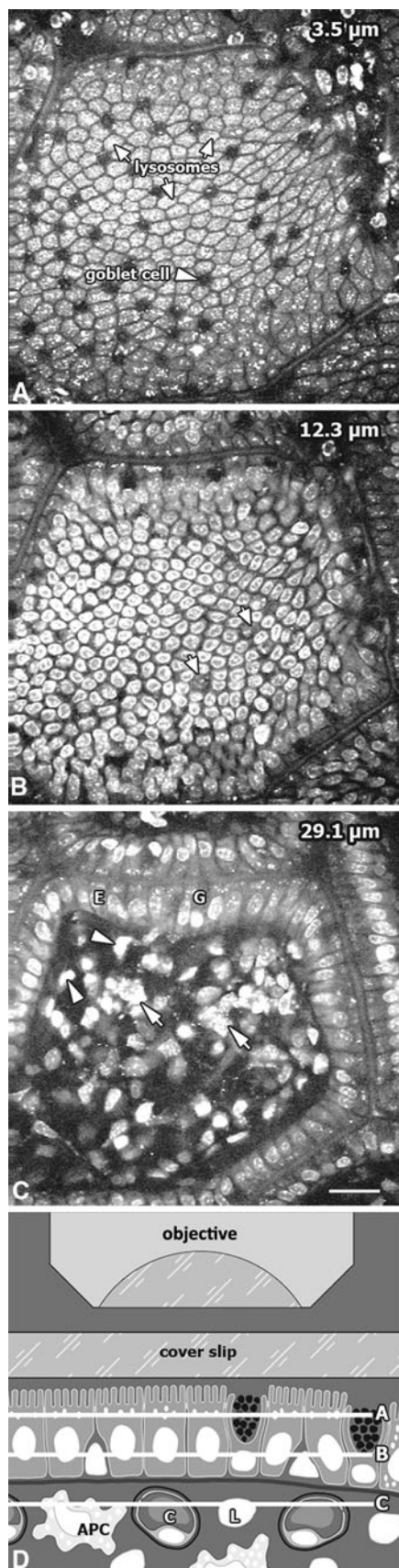
section. UEA-I FITC lectin also selectively bound to the brush border of brush cells in preserved tissue. *Green*, UEA-I FITC; *blue*, nuclei (*n*) stained with Hoechst 33258 dye; *dark gray*, DIC. **c** On-section lectin labeling of brush cells with UEA-I using 20-nm colloidal gold to localize binding sites. The microfilament rootlet bundles extend deeply into the apical cytoplasm. (Scale bars **a, b** 5 μm ; **c**, 1 μm)

moved forward. In six experiments analyzed in detail, 440 lymphocytes in the lamina propria were tracked and they displayed an average velocity of $11.8 \pm 4.7 \mu\text{m min}^{-1}$, with peak velocities that exceeded $24 \mu\text{m min}^{-1}$.

Discussion

Intravital microscopy is a powerful method for studying fundamental issues of physiology and in vivo morphology.

It is currently performed in a variety of organs including brain (Trachtenberg et al. 2002), lymph nodes (Mempel et al. 2004), skin (Masters and So 1999) and kidney (Dunn et al. 2002) and is mostly based on fluorescent dyes introduced to individual cells of interest. Autofluorescence 2-photon (A2P) microscopy, as introduced in this paper, opens a new window which enables time-resolved in vivo histology and physiology of the small intestinal mucosa without the need to add fluorescent stains. Using a high aperture objective (40/1.2), we reach a 0.5-micron



◀ **Fig. 7** Images of a 29.1- μm -thick stack of mouse small intestine excited at 730 nm 24 h after intravenous application of Hoechst 33258. Stack of optical sections through a villus: **a** in 3.5 μm below the tissue surface, highly fluorescent lysosomes (*arrows*) and mitochondrial NAD(P)H in the apical cytoplasm of enterocytes exhibited a strong signal. Mucus-containing goblet cells (*arrowhead*) appeared dark **b** in 12.3- μm depth, the image predominantly showed the nuclei of enterocytes, which had assimilated the Hoechst dye. Nuclei of goblet cells (*arrows*). **c** In 29.1- μm depth, the underlying lamina propria was identified. The nuclei of most contained cells assimilated the Hoechst dye. Lymphocytes, which usually show only weak fluorescence exhibited a strong labeling (*arrowheads*). Antigen-presenting cells (APC) were recognized by their strongly fluorescent lysosomes (*arrows*). Enterocyte (E), goblet cell (G) **d** schematic diagram of the three different focus planes (**a–c**) shown above. Lymphocyte (L), capillary (C), antigen presenting cell (APC). (*Scale bar*, 20 μm)

resolution so that our approach by far exceeds the resolution of previous intravital studies of the intact intestine (Watson et al. 2005) and vivo imaging is no longer restricted to the cellular level, but extends to subcellular organelle-based imaging of processes such as endocytosis. The greatest advantage of intravital A2P microscopy is the fact that the viability of the tissue is maintained and all tissue elements can be visualized in our experimental setup. The intestine is surgically exposed, but with intact circulatory connections. This was demonstrated by erythrocyte movement phenomena and vigorously moving lymphocytes in the villus lamina propria (Fig. 8, Online Resource ESM_3.mpg). Staining with fluorescent probes and repeated image acquisition did not affect viability (Figs. 6, 7, 8).

A2P microscopy opens a new window for investigating cellular and subcellular dynamics of immune processes within the mucosa of the small intestine. The lamina propria is a loose connective tissue underlying the epithelium and contains numerous immune cells which are considered critical in maintaining the balance between the immune response against harmful pathogens and the induction of tolerance to commensal bacteria and food antigens. Macrophages are the most abundant population of phagocytic cells in the intestine of humans (Lee et al. 1985), demonstrate inflammatory anergy (Smythies et al. 2005) and are assumed to have important functions in maintaining mucosal tolerance. Recent advances have highlighted also a fundamental role for lamina propria dendritic cells, which are highly abundant in rodents, in this function (Uematsu et al. 2008; Varol et al. 2009). Antigen presenting cells (APCs) such as macrophages and dendritic cells give a strong signal in A2P microscopy (Figs. 3, 7, Online Resource, ESM_1.mpg, Online Resource ESM_2.mpg) because they harbor numerous lysosomes, which can easily be distinguished from mitochondria by excitation wavelength and fluorescence lifetime imaging (Fig. 5). Lamina

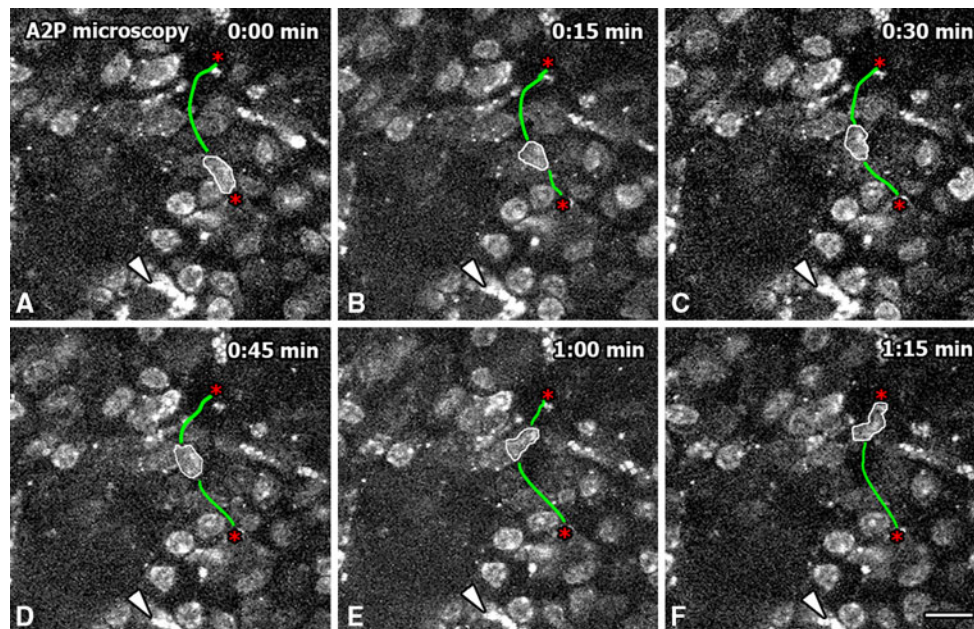


Fig. 8 a–f Time-lapse series of the lamina propria of mouse small intestine excited at 730 nm 24 h after intraperitoneal application of Hoechst 33258. Individual lymphocytes assimilated the Hoechst dye and could easily be identified by their stained nuclei. Using time-lapse 3D imaging, we visualized cell motility of single lymphocytes (white

outline) up to 40 min. (Here shown a period of 1 min and 15 s). Lymphocytes in the lamina propria displayed average velocities of $12 \mu\text{m min}^{-1}$. Red asterisks mark start and end point of the track (green). Antigen presenting cell (arrowheads). (Scale bar 10 μm)

propria lymphocytes (LPL) are also a dominant cell population in the subepithelial tissue and display a phenotype separate from peripheral blood T cells (MacDonald and Pender 1998). Apparently, LPL also play an important role in keeping the immunological homeostasis at the large resorptive interface between the gut lumen and the interior of the body. Our current understanding of immune cell motility and migration in the lamina propria of small intestinal mucosa derives from indirect evidence (Mahida et al. 1997), because it has not been possible to observe these dynamic processes in vivo so far. In the present study, we injected a nuclear dye intraperitoneally 24 h prior to 2-photon microscopy. It is known that lymphatic drainage of the peritoneal cavity takes place toward the mediastinal lymph nodes, prior to systemic dissemination (Marco et al. 1992). We assume that after lymphatic drainage of the dye into the mediastinal lymph nodes, some lymphocytes within the lymph node strongly assimilated the nuclear dye and then migrated into the lamina propria of the small intestine. Morphological aspects and velocities of labeled cells make it most likely that these cells are lymphocytes, which are found to a relatively high proportion in the lamina propria of the small intestinal mucosa and are mostly CD4+, TCR- $\alpha\beta$ + cells (Resendiz-Albor et al. 2004). For the first time, we could analyze the motility of individual labeled lymphocytes within the lamina propria of the small intestine using time-lapse, three

dimensional imaging (Fig. 8, Online Resource ESM_3.mpg). The average velocity of $11.8 \pm 4.7 \mu\text{m min}^{-1}$, with peak velocities that exceeded $24 \mu\text{m min}^{-1}$ correlates well with measurements of lymphocytes in intact lymph nodes (Miller et al. 2002). Primary lymphocyte responses require contact-dependent information exchange between lymphocytes and dendritic cells (Mempel et al. 2004). In time series, we observed direct dynamics of lymphocyte–APC interactions (Online Resource ESM_3.mpg), so that applying this technology for visualization of immune cell interactions in intact intestinal mucosa will open a new angle of view on the events involved in antigen-specific immune reactions in the gut. Understanding how immune cells search for pathogens in the intestine is a critical area in which intravital microscopy will probably be the key technology. Creative use of pathogen genetics, mouse genetics and imaging technology, with attention to physiological modes of infection and careful data analysis and modeling, is likely to provide new insights leading to new approaches to combat infections.

The use of A2P microscopy for intravital studies of the intestine, as described in this paper, provides a powerful tool for evaluating tissue histology and cell biology in the most physiologically relevant setting. Our study demonstrates numerous ways how A2P microscopy can be applied to various aspects of intestinal biology and physiology to investigate the complexity and the dynamics of

cellular environments with intact circulatory and nervous connections.

Acknowledgments This study was supported by the German research foundation (DFG), Projects No. Ge 647/9-1; Ge 647/10-1; HU 629/3-1; HU 629/4-1). We thank H. Manfeldt and C. Öriin for excellent technical assistance.

Open Access This article is distributed under the terms of the Creative Commons Attribution Noncommercial License which permits any noncommercial use, distribution, and reproduction in any medium, provided the original author(s) and source are credited.

References

- Bennett BD, Jetton TL, Ying G, Magnuson MA, Piston DW (1996) Quantitative subcellular imaging of glucose metabolism within intact pancreatic islets. *J Biol Chem* 271:3647–3651
- Caldwell CC, Kojima H, Lukashev D, Armstrong J, Farber M, Apasov SG, Sitkovsky MV (2001) Differential effects of physiologically relevant hypoxic conditions on T lymphocyte development and effector functions. *J Immunol* 167:6140–6149
- Denk W, Strickler JH, Webb WW (1990) Two-photon laser scanning fluorescence microscopy. *Science* 248:73–76
- Dunn KW, Sandoval RM, Kelly KJ, Dagher PC, Tanner GA, Atkinson SJ, Bacallao RL, Molitoris BA (2002) Functional studies of the kidney of living animals using multicolour two-photon microscopy. *Am J Physiol* 283:905–916
- Gebhard A, Gebert A (1999) Brush cells of the mouse intestine possess a specialized glycocalyx as revealed by quantitative lectin histochemistry: further evidence for a sensory function. *J Histochem Cytochem* 47:799–808
- Hall PA, Coates PJ, Ansari A, Hopwood D (1994) Regulation of cell number in the mammalian gastrointestinal tract: the importance of apoptosis. *J Cell Sci* 107:3569–3577
- Harding CV, Collins DS, Slot JW, Geuze HJ, Unanue ER (1991) Liposome-encapsulated antigens are processed in lysosomes, recycled, and presented to T cells. *Cell* 64:393–401
- Hoefler D, Puschel B, Drenckhahn D (1996) Taste receptor-like cells in the rat gut identified by expression of α -gustducin. *Proc Natl Acad Sci USA* 93:6631–6634
- Huang SH, Heikal AA, Webb WW (2002) Two-photon fluorescence spectroscopy and microscopy of NAD(P)H and flavoprotein. *Biophys J* 82:2811–2825
- Koenig K (2000) Multiphoton microscopy in life sciences. *J Microsc* 200:83–104
- Lee SH, Starkey PM, Gordon S (1985) Quantitative analysis of total macrophage content in adult mouse tissues. Immunohistochemical studies with monoclonal antibody F4/80. *J Exp Med* 161:475–489
- MacDonald TT, Pender SL (1998) Lamina propria T cells. *Chem Immunol* 71:103
- Mahida YR, Galvin AM, Gray T, Makh S, McAlindon ME, Sewell HF, Podolsky DK (1997) Migration of human intestinal lamina propria lymphocytes, macrophages and eosinophils following the loss of surface epithelial cells. *Clin Exp Immunol* 109:377–386
- Marco AJ, Domingo M, Ruberte J, Carretero A, Briones V, Dominguez L (1992) Lymphatic drainage of *Listeria monocytogenes* and Indian ink inoculated in the peritoneal cavity of the mouse. *Lab Anim* 26:200–205
- Masters BR, So PT (1999) Multi-photon excitation microscopy and confocal microscopy imaging of in vivo human skin: a comparison in vivo. *Microsc Microanal* 4:282–289
- Mempel TR, Henrickson SE, von Andrian UH (2004) T-cell priming by dendritic cells in lymph nodes occurs in three distinct phases. *Nature* 427:154–159
- Miller MJ, Wei SH, Parker I, Cahalan MD (2002) Two-photon imaging of lymphocyte motility and antigen response in intact lymph node. *Science* 296:1869–1873
- Patterson GH, Knobel SM, Arkhammar P, Thastrup O, Piston DW (2000) Separation of the glucose-stimulated cytoplasmic and mitochondrial NAD(P)H responses in pancreatic islet β cells. *Proc Natl Acad Sci USA* 97:5203–5207
- Peters PJ, Raposo G, Neefjes JJ, Oorschot V, Leijendekker RL, Geuze HJ, Ploegh HL (1995) Major histocompatibility complex class II compartments in human B lymphoblastoid cells are distinct from early endosomes. *J Exp Med* 182:325–334
- Piston DW, Knobel SM (1999) Quantitative imaging of metabolism by two-photon excitation microscopy. *Methods Enzymol* 307:351–368
- Resendiz-Albor AA, Esquivel R, Lopez-Revilla R, Verdin L, Moreno-Fierros L (2004) Striking phenotypic and functional differences in lamina propria lymphocytes from the large and small intestine of mice. *Life Sci* 76:2783–2803
- Schmidt H, Gelhaus C, Lucius R, Nebendahl M, Leippe M, Janssen O (2009) Enrichment and analysis of secretory lysosomes from lymphocyte populations. *BMC Immunol* 10:41
- Shin H-J, Mego J-L (1988) A rat liver lysosomal membrane flavin-adenine dinucleotide phosphohydrolase: purification and characterization. *Arch Biochem Biophys* 267:95–103
- Skala MJ, Ricking KM, Fitzpatrick AG, Eickhoff J, Eliceiri KW, White JG, Ramanujam N (2007) In vivo multiphoton microscopy of NADH and FAD redox states, fluorescence lifetimes, and cellular morphology in precancerous epithelia. *PNAS* 104:19494–19499
- Smythies LE, Sellers M, Clements RH, Mosteller-Barnum M, Meng G, Benjamin WH, Orenstein JM, Smith PD (2005) Human intestinal macrophages display profound inflammatory anergy despite avid phagocytic and bacteriocidal activity. *J Clin Invest* 115:66–75
- Stoll S, Delon J, Brotz TM, Germain RN (2002) Dynamic imaging of T cell–dendritic cell interactions in lymph nodes. *Science* 296:1873–1876
- Strater J, Koretz K, Günther AR, Möller P (1995) In situ detection of enterocytic apoptosis in normal colonic mucosa and in familial adenomatous polyposis. *Gut* 37:819–823
- Trachtenberg JT, Chen BE, Knott GW, Feng G, Sanes JR, Welker E, Svoboda K (2002) Long-term in vivo imaging of experience-dependent synaptic plasticity in adult cortex. *Nature* 420:788–794
- Tulp A, Verwoerd D, Dobberstein B, Ploegh HL, Pieters J (1994) Isolation and characterization of the intracellular MHC class II compartment. *Nature* 369:120–126
- Uematsu S, Fujimoto K, Jang MH, Yang BG, Jung YJ, Nishiyama M, Sato S, Tsujimura T, Yamamoto M, Yokota Y, Kiyono H, Miyasaka M, Ishii KJ, Akira S (2008) Regulation of humoral and cellular gut immunity by lamina propria dendritic cells expressing Toll-like receptor 5. *Nat Immunol* 9:769–776
- Varol C, Vallon-Eberhard A, Elinav E, Aychek T, Shapira Y, Luche H, Fehling HJ, Hardt WD, Shakhar G, Jung S (2009) Intestinal lamina propria dendritic cell: subsets have different origin and functions. *Immunity* 31:502–512
- von Andrian UH (2002) T cell activation in six dimensions. *Science* 296:1815–1817
- Watson AJM, Chu S, Sieck L, Gerasimenko O, Bullen T, Campbell F, McKenna M, Rose T, Montrose M (2005) Epithelial barrier function in vivo is sustained despite gaps in epithelial layers. *Gastroenterology* 129:902–912